Applying the new experimental midpoint concept on strain energy density for fracture assessment of composite materials

Khaji, Zahra; Fakoor, Mahdi; Manafi Farid, Hannaneh; Alderliesten, René

DOI
10.1016/j.tafmec.2022.103522

Publication date
2022

Document Version
Final published version

Published in
Theoretical and Applied Fracture Mechanics

Theoretical and Applied Fracture Mechanics 121 (2022) 103522

Contents lists available at ScienceDirect

Theoretical and Applied Fracture Mechanics

journal homepage: www.elsevier.com/locate/tafmec

Applying the new experimental midpoint concept on strain energy density for fracture assessment of composite materials

Zahra Khaji [a], Mahdi Fakoor [a,*], Hannaneh Manafi Farid [b], René Alderliesten [c]

[a] Faculty of New Sciences and Technologies, University of Tehran, Tehran, Iran
[b] Department of Mechanical Engineering, University of Alberta, Edmonton, Alberta, Canada
[c] Structural Integrity & Composites Group, Faculty of Aerospace Engineering, Delft University of Technology, Kluyverweg 1, 2629HS Delft, The Netherlands

ARTICLE INFO

Keywords:
Minimum strain energy density
Orthotropic materials
Midpoint of experimental data
Crack initiation angle

ABSTRACT

A mixed-mode I/II fracture criterion for predicting the fracture response of composite materials is proposed. This criterion is derived based on a comprehensive study and the consideration of the physics of fracture onset. The fracture phenomenon that causes the various damage mechanisms at the vicinity of the crack tip is examined. It is elucidated that the stress distribution at the crack tip ought to be defined using the reinforcement isotropic solid (RIS) stress state. This new criterion, which is called Improved Strain Energy Density with Mid-point (ISEDM), includes the effect of the fracture process zone (FPZ) and *T*-stress, which remarkably affect the mixed-mode fracture process, particularly, when mode II is dominant. Substituting the strain energy density in a pure mode I with the strain energy density in the midpoint of mixed-mode I/II is the creative idea employed in proposing this criterion. Because in pure mode I the effects of FPZ are minimal, change of fitting point on fracture limit curve (FLC) from K_{Ic} to midpoint critical stress intensity factors (CSIF's) makes it possible to consider the effects of FPZ more accurately. In the ISEDM criterion, fracture behavior depends on mechanical properties and CSIF's of the midpoint. Crack initiation angle is considered along minimum strain energy density and this angle is derived in the midpoint of mixed-mode I/II. RIS theory is used as an applicable theory for modeling orthotropic materials in this paper and causes valid and reliable fracture behavior to be extracted. In addition, changing fracture point from pure mode I to the mid-point of experimental data causes the effects of FPZ to be considered without estimating the toughening mechanisms in this zone, and the fracture behavior is extracted with higher accuracy. FLC's in comparison with available experimental data prove that the ISEDM criterion anticipates the fracture behavior of orthotropic materials well. Finding K_{IIc} based on the analytical method is a valuable achievement. In this article, K_{IIc} can be predicted with appropriate accuracy, only by CSIF's of mid-point and using ISEDM criterion.

1. Introduction

Composite materials are widely used in the aerospace industry owing to their low weight and high specific strength and stiffness [1]. The number of experimental, theoretical, and numerical studies on the composite materials subjected to various loading shed light on the significance of these materials in industrial applications [2–9]. Creating different defects in the composite structures increases the possibility of failure in these materials [10]. Therefore, achieving an efficient fracture criterion is essential to predict the fracture response of these materials. As a result, a great number of researches have been conducted in order to evaluate the fracture behavior [11,12]. The issue of designing and predicting the fracture behavior of structures is one of the most important issues that scientists have addressed. Many studies have been performed to predict the fracture behavior of structures [13–20]. In addition, the estimation of fracture toughness in pure mode I [21,22], pure mode II [23], pure mode III [24,25], mixed-mode I/II [26,27], and mixed-mode I/III [28,29] is one of the most important topics in the fracture mechanics field. Many researchers experimentally predict the values of fracture toughness by performing experimental tests on different specimens. The amount of fracture toughness can be theoretically predicted based on a specific criterion [30–32]. They evaluated their predictions by comparing them with experimental values.

The fracture criteria are presented based on stress or energy to assess the fracture response of isotropic and orthotropic materials. Maximum

* Corresponding author.
E-mail address: mfakoor@ut.ac.ir (M. Fakoor).

https://doi.org/10.1016/j.tafmec.2022.103522
Received 16 March 2022; Received in revised form 23 June 2022; Accepted 29 July 2022
Available online 1 August 2022

Nomenclature

K	Stress intensity factor
K_I,K_{II}	Mode I and II stress intensity factors
K_{Ic},K_{IIc}	Mode I and II fractrue toughness
K_{I_M},K_{II_M}	Mode I and II stress intensity factors of midpoint
G	Maximum strain energy release rate
G_{Ic},G_{IIc}	Maximum strain energy release rate for pure mode I and II
$(G_{IIc})_{SED}$	Maximum strain energy release rate for pure mode II derived based on the relation of strain energy density and strain energy release rate
$(G_{IIc})_{ENF}$	Maximum strain energy release rate for pure mode II derived by conducting a test on End-Notch Flexure specimens
S	Strain energy density factor
S_{Ic},S_{IIc}	Critical strain energy density factor for pure mode I and II
T	T-stress
c_{ij}	Compliance components of the composite material in the on-axis coordinate system
E_{xx},E_{yy}	Elastic module of laminated composite along the fiber and across the fiber
ν,ν_{xy},ν_{yx},ν_m	Poisson's ratio, Poisson's ratio in the plane xy, Poisson's ratio of the isotropic matrix
V_f	The volume fraction of fibers
σ_{ij}^{Iso},σ_{ij}^{orth}	Stress state of the crack tip of the isotropic and orthotropic materials
σ_c	The strength of (the isotropic matrix) material
ξ_i	Reinforcement coefficients or ReSt factors in the on-axis coordinate system
f_{ij},g_{ij}	Angular functions of the stress state in the vicinity of the crack
r,θ	Polar distance from the crack tip, Polar angle
r_c,θ_c	Critical distance and angle where the crack growth occur

tangential stress [33,34], maximum strain energy release rate [35], and minimum strain energy density [36,37] criteria are proposed for isotropic materials.

Jernkvist [38] developed SER, SED, and maximum principle stress (MPS) criteria by considering the crack growth in orthotropic materials along the fibers [39] and investigated mixed-mode fracture for crack along and across fibers.

Based on Van der Put's theory, Fakoor et al. proposed a new concept called the "reinforcement isotropic solid" (RIS) model for assessment of crack behavior of orthotropic materials under mixed-mode I/II loading [40–42]. The main assumption of the RIS model is that orthotropic material is considered as an isotropic material that is reinforced with fibers. Applying the RIS concept to the conventional fracture criteria of isotropic materials (such as SED, MTS, and SER) allows the development of these criteria for orthotropic materials. The validity of the proposed fracture criteria for orthotropic materials based on RIS is evaluated with experimental test results [43–47].

Recently, it is proven that the fracture process zone (FPZ) significantly influences the fracture process of composite materials [48–54]. In the FPZ, several mechanisms such as the nucleation of micro-cracks cause the dissipation of energy and prevent catastrophic failure [55–59]. The effects of the FPZ, where micro-cracks nucleate and propagate, have been studied and a criterion derived based on dissipated energy in the FPZ [60]. Given the fracture toughness based on the maximum strain energy release rate (SERR), a rather accurate approximation of fracture based on the fracture mechanics becomes possible [61]. The micro-mechanics approach to study the fracture behavior displayed a fine description of the fracture process.

By investigating the micro-crack distribution in FPZ, using the development of nonlocal stress criterion, Romanowicz & Seweryn [48] presented a novel criterion to assess the crack behavior of cracked wooden materials under mixed-mode I/II loading. Based on the relationship between the properties of undamaged and damaged solid, a model for the damaged zone can be developed [51]. The shape, size and density of the microcracks affect the properties of the damaged zone. Using the properties of the damaged material, the fracture behavior of the material can be predicted with acceptable accuracy [49].

Dissipated energy in the crack initiation phase is used to create a damaged zone around the crack tip. To create microcracks and other nonlinear mechanisms such as plastic deformation, significant damage occurs in this phase [62]. In the crack propagation phase, a weak zone called fiber bridge is created around the crack tip. This mechanism is related to non-broken fibers bridging when crack exists [59]. As the crack length increases, the bridging becomes weaker until the separation of the fracture surfaces occurs [63]. This mechanism has an important effect on the mixed-mode fracture behavior. The FPZ delays the fracture of specimens by absorbing strain energy. In addition, it prevents catastrophic failure [64].

A great number of scholars attempted to interlink the macroscopic fracture and the microscopic damage of composite materials through SERR [65–71]. It is observed that the maximum energy release rate for pure mode I and II is not identical. For mode II, the energy release rate is reported much higher than mode I. To thoroughly consider the physics of fracture more studies are carried out [72,73]. It is examined that accurate approximation is possible when the fracture model explicitly includes the physical procedure of the materials. Therefore, they related the toughness of materials to the energy release rate by the SED criterion [74]. These studies clearly show that microscopic behavior is well established to predict the macroscopic behavior of fractures. However, the discrepancy between their model and experimental study is remarkable. They considered that the principal reason for this discrepancy is that the derived G_{IIc} by experimental study measured the energy dissipated for the occurrence of the other damage factors ahead of the crack tip before the propagation of the crack so that G_{IIc} does not indicate the crack initiation, while G_{Ic} measures the initiation of the crack growth. However, it is noteworthy that in composite materials, the crack initiates and propagates in the matrix. Therefore, the crack onset and growth occur in the matrix, which is isotropic material. This phenomenon thoroughly examined and proved that criteria based on the reinforced isotropic solid (RIS) improved the prediction of crack growth at the orthotropic materials [40,42,44,45,63,75–77].

In this study, it is assumed that the crack initiation and propagation take place in the isotropic matrix reinforced. The ratio of the fracture toughness of composite materials, K_{Ic} andK_{IIc}, is obtained based on the SED criterion and related to the ratio of G_{Ic} andG_{IIc}, respectively. Also, the effect of T-stress at the crack tip at the fracture process is discussed. In addition, the well-known SED criterion is extended to predict the crack behavior of composite materials. In this paper, critical stress intensity factors in the midpoint are substituted to the fracture toughness at mode I that is prevalent in the previous fracture criteria. The validity of this criterion is evaluated by comparing FLC's with the available experimental data. As a result, the proposed fracture criterion dominantly envelopes the influence of mode II that plays the chief role in the dissipation of the energy. The proposed criterion, consequently, well-explain the discrepancy between the prediction of crack growth based on G_{Ic} andG_{IIc}.

2. Reinforced isotropic solid (RIS) concept

In the macroscopic framework, the failure of composite materials

under mixed-mode loading is studied based on the linear elastic fracture mechanics (LEFM) [37–39]. In these studies, several renowned isotropic criteria [35,78,79] are extended to anisotropic materials using the anisotropic stress state [80]. Extremely helpful as these criteria are, they are too conservative and are not able to be applied for industrial engineering applications. As a remarkable result of this study, some research has been done to improve the extended criteria [40,42,44,48–51,76,77,81,82].

To derive a correct failure criterion that describes the fracture behavior of orthotropic materials with unidirectional fibers such as wood, it is demonstrated that orthotropic materials ought to care as a reinforced matrix [83]. It is mathematically proven that the Airy stress functions of orthotropic materials do not satisfy the equilibrium conditions and strength criterion of the matrix, as determining elements in the matrix cracking. Therefore, the Airy stress function is solved for the isotropic matrix [74]. As a result, other research has been conducted to evaluate matrix cracking at orthotropic materials [74]. It is concluded that the cracks embedded in the matrix initiate and propagate in the isotropic medium, while it is significantly affected by the fibers. The matrix of the orthotropic materials, thus, is referred to as reinforcement isotropic solid (RIS). The isotropic solid is reinforced by fibers and displays more vigorous strength behavior at the crack tip. In this kind of materials, the airy stress function of orthotropic materials transfers to the airy stress function of the isotropic materials, while the influence of the fibers on the matrix is regarded. In the other words, based on the RIS concept, the isotropic stress state is substituted for the anisotropic stress state of the crack tip, while including several coefficients that attributed to the reinforcement effect of fibers on the matrix. Numbers of studies recently have been carried out to study the coefficients to improve the fracture criteria [43–45,49,75–77]. As a result of the RIS concept, the theoretical relation between the mode I and II toughness and energy release rate is obtained [74]. Also, based on various fracture criteria, the theoretical relation between K_{Ic} andK_{IIc},which is called damage factor, is obtained to facilitate deriving the value of the K_{IIc} according to theK_{Ic}. The importance of establishing accurate theoretical relationship between K_{Ic} andK_{IIc}, or damage factor, is to avoid the practically arduous and equally costly experimental tests to deriveK_{IIc}, which are approximately impossible to achieve the correct value [40,42,44,48–51,76,77,82].

Based on the RIS theory, the stress state of the crack tip defines as below [44,74]:

$$\xi_1 = \frac{\sigma_{11}^{Iso}}{\sigma_{11}^{Orth}} \tag{1}$$

$$\xi_2 = \frac{\sigma_{22}^{Iso}}{\sigma_{22}^{Orth}} \tag{2}$$

$$\xi_3 = \frac{\sigma_{12}^{Iso}}{\sigma_{12}^{Orth}} \tag{3}$$

Where ξ_i are called the Reduced Stress coefficients (ReSt coefficients) that are derived based on RIS theories [44].

To generally study the fracture of composite materials, it is assumed that they are subjected to mixed mode I/II loading. Therefore, it is required to derive a failure model and criteria which anticipate the crack growth of anisotropic materials under mixed-mode loadings. Strain energy stores in the structure when it is subjected to loading. The imposed energy starts to de-cohesion the materials by initiation and propagation of the crack when the strain energy reaches the critical value at a certain local. Therefore, the strain energy density criterion is employed to derive the criterion which not only is based on the energy dissipation in the structure but also regards the stress distribution at the crack tip, which plays a significant role in determining the damage mechanism in fracture [66,84,85].

ReSt coefficients are defined as follow [75]:

$$\xi_1 = \frac{E_1}{E_2} \tag{4}$$

$$\xi_2 = 1 \tag{5}$$

$$\xi_3 = (1 - V_f)(1 + \frac{E_{11}(1 + \nu_{21})}{E_{22}(1 + \nu_{12})}) \tag{6}$$

The stress state at the crack tip in isotropic materials is [86]:

$$\sigma_{11}^{Iso} = \frac{f_{11}(\theta)K_I + g_{11}(\theta)K_{II}}{\sqrt{2\pi r}} \tag{7}$$

$$\sigma_{22}^{Iso} = \frac{f_{22}(\theta)K_I + g_{22}(\theta)K_{II}}{\sqrt{2\pi r}} \tag{8}$$

$$\sigma_{12}^{Iso} = \frac{f_{12}(\theta)K_I + g_{12}(\theta)K_{II}}{\sqrt{2\pi r}} \tag{9}$$

In which,$f_{ij}(\theta)$ and $g_{ij}(\theta)$ are angular functions of isotropic materials and are written in Appendix A. Fig. 1 shows the stress field around the crack tip in an orthotropic material under mixed mode I/II loading. The crack is along the fibers and is located between the fibers in the matrix section. Because the matrix is weaker than the fibers, the crack propagates along the fibers. Based on the RIS concept and ReSt coefficients in Eqs (4)-(6), the stress state at the crack tip in orthotropic materials is [87]:

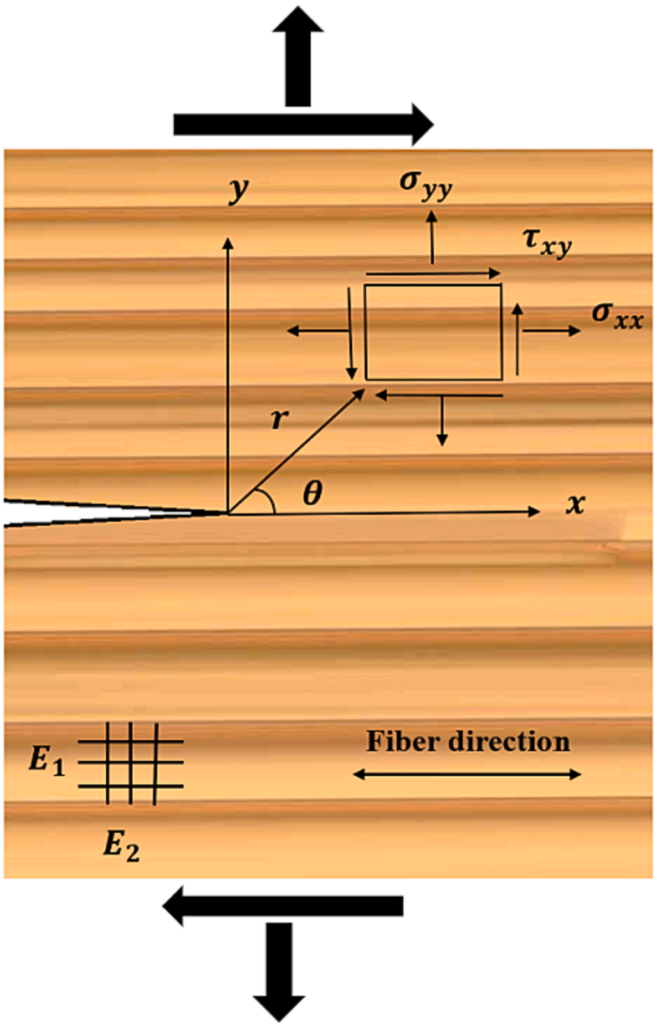

Fig. 1. Stress field around crack tip for orthotropic materials.

$$\sigma_{11}^{Orth} = \frac{f_{11}(\theta)K_I + g_{11}(\theta)K_{II}}{\xi_1\sqrt{2\pi r}} \tag{10}$$

$$\sigma_{22}^{Orth} = \frac{f_{22}(\theta)K_I + g_{22}(\theta)K_{II}}{\xi_2\sqrt{2\pi r}} \tag{11}$$

$$\sigma_{12}^{Orth} = \frac{f_{12}(\theta)K_I + g_{12}(\theta)K_{II}}{\xi_3\sqrt{2\pi r}} \tag{12}$$

Regarding Eqs. 10–12, extended minimum strain energy density (ESED) is as follows[88]:

$$S_c = A_{11}(\theta)K_I^2 + 2A_{12}(\theta)K_IK_{II} + A_{22}(\theta)K_{II}^2 \tag{13}$$

In which:

$$A_{11} = \frac{1}{4\pi}\left(\frac{C_{11}}{\xi_1^2}f_{11}^2 + \frac{C_{22}}{\xi_2^2}f_{22}^2 + \frac{C_{66}}{\xi_3^2}f_{12}^2 + 2\frac{C_{12}}{\xi_1\xi_2}f_{11}f_{22}\right) \tag{14}$$

$$A_{12} = \frac{1}{4\pi}\left(\frac{C_{11}}{\xi_1^2}f_{11}g_{11} + \frac{C_{22}}{\xi_2^2}f_{22}g_{22} + \frac{C_{66}}{\xi_3^2}f_{12}g_{12} + \frac{C_{12}}{\xi_1\xi_2}(f_{11}g_{22} + f_{22}g_{11})\right) \tag{15}$$

$$A_{22} = \frac{1}{4\pi}\left(\frac{C_{11}}{\xi_1^2}g_{11}^2 + \frac{C_{22}}{\xi_2^2}g_{22}^2 + \frac{C_{66}}{\xi_3^2}g_{12}^2 + 2\frac{C_{12}}{\xi_1\xi_2}g_{11}g_{22}\right) \tag{16}$$

The critical strain energy density factor defines as $S = S_c$ at the crack tip when the specimen is subjected to pure mode I [89].

S_{Ic} is pertinent to pure mode I, when$K_I = K_{Ic}$,$K_{IIc} = 0$, and$\theta_c = 0$. Therefore, $S_{Ic} = A_{11}(0)K_{Ic}^2$ in which:

$$A_{11}(0) = \frac{1}{4\pi}\left(\frac{C_{11}}{\xi_1^2} + \frac{C_{22}}{\xi_2^2} + 2\frac{C_{12}}{\xi_1\xi_2}\right) \tag{17}$$

And:

$$S_{Ic} = \frac{1}{4\pi}\left(\frac{C_{11}}{\xi_1^2} + \frac{C_{22}}{\xi_2^2} + 2\frac{C_{12}}{\xi_1\xi_2}\right)K_{Ic}^2 \tag{18}$$

S_{Ic} depends on the material properties, fracture toughness, and fiber fraction of the composites. θ_c is obtained by solving the sets of two following equations, and equals to the crack growth path at isotropic materials [88].

$$\frac{\partial A_{11}(\theta)}{\partial\theta}K_I^2 + 2\frac{\partial A_{12}(\theta)}{\partial\theta}K_IK_{II} + \frac{\partial A_{22}(\theta)}{\partial\theta}K_{II}^2 = 0 \tag{19}$$

$$\frac{\partial^2 A_{11}(\theta)}{\partial\theta^2}K_I^2 + 2\frac{\partial^2 A_{12}(\theta)}{\partial\theta^2}K_IK_{II} + \frac{\partial^2 A_{22}(\theta)}{\partial\theta^2}K_{II}^2 > 0 \tag{20}$$

Eq. (13) in pure mode II is restated as follows:

$$K_{Ic}^2 = \frac{A_{22}(\theta_c)}{A_{11}(0)}K_{IIc}^2 \tag{21}$$

Where damage factorρ, for ESED criterion is defined as.

$$\rho = \frac{K_{Ic}^2}{K_{IIc}^2} = \frac{A_{22}(\theta_c)}{A_{11}(0)} \tag{22}$$

In pure mode I, $\theta_c = 0$ and the damage factor is:

$$\rho = \frac{C_{66}}{\xi_3^2\left(\frac{C_{11}}{\xi_1^2} + C_{22} + 2\frac{C_{12}}{\xi_1}\right)} \tag{23}$$

One should notice that based on the RIS concept all properties including elastic properties and toughness in fracture of composite materials are pertinent to the isotropic matrix where the crack initiates and propagates. In the previous research, damage factor is derived for various criteria [39,40,44,48–50,75,77,81,90,91]. Table 1 reports the mechanical properties of all wood specimens used in this article. Table 2 indicates the criteria and the value of ρ i.e. the ratio of K_{Ic} to K_{IIc} for various types of wood.

The first row of Tables 2 and 3 contain the damage factor derived by [48], which demonstrated the ratio of the stress intensity factors for pure mode I and II based on the experimental study. This factor is extracted based on the micro-crack density and the actual micro-crack size, thus it is the real ratio. Comparing the value of the damage factor derived based on LEFM [39] to the damage factor of criteria based on the RIS concept [39,49,75,91], it is concluded that the RIS concept improves the prediction of the K_{IIc} based on K_{Ic} using different criteria. It means that the RIS concept is remarkably capable of describing the physics-based theory of the fracture of composite materials. The strength approach estimated the damage factor with high accuracy because the effect of FPZ around the crack tip is considered in the extraction of the damage factor.

3. ESED criterion considering the effect of *T*-stress term

When fracture occurs in the composite material, the cracks growth in the reinforced isotropic matrix following the RIS theory. However, it is well established that the crack grows along a direction that maximum energy release rate occurs, consequently, the crack does not co-linearly distribute at mixed-mode loading [44]. In this case, therefore, it is well established that *T*-stress significantly exerts an influence on the fracture behavior of the materials. Consequently, the *T*-stress term is required to be taken into account in the stress state at the crack tip. Some research has been conducted to propose a criterion based on the description of the stress state at the vicinity of the crack tip. It is comprehensively discussed that several phenomena at fracture mechanics are associated with *T*-stress [92]. The stress distribution around the crack tip for pure mode I is widely different from stress distribution for the pure mode II although the stress level for both is similar [93]. It is well-known that the *T*-stress value is constant and independent of the distance from the crack tip. It can be concluded that in mixed mode loading when mode II is dominant, *T*-stress affects the damage mechanisms in the vicinity of the crack tip. It means that for a fracture criterion for mixed-mode loading to be accurate and based on the physical phenomena of the fracture procedure, it must include the *T*-stress. Accordingly, in the SED criterion, the *T*-stress term is taken into the consideration at the stress state of the crack tip, and subsequently, at the fracture criterion. The Extended strain energy Density criterion (ESED) is stated as the following equation.

Table 1
The mechanical properties for various wooden materials.

Composite material	$E_L(Gpa)$	$E_T(Gpa)$	$E_R(Gpa)$	$G_{LR}(Gpa)$	ν_{LT}	ν_{RT}	ν_{LR}
Scots-Pine [38]	16.3	0.57	1.1	1.74	0.56	0.34	0.47
Norway-Spruce [39]	11.84	0.64	0.81	0.63	0.56	0.34	0.38
Red-Spruce [38]	12.7	0.63	0.98	0.8	0.42	0.37	0.3
Im7/977–2 [72]	143	9.2	9.2	4.8	0.3	0.3	0.5
IM7/8552 [72]	165	9	9	5.6	0.34	0.34	0.5
AS4/3501–6 [72]	132	9.7	9.7	5.9	0.28	0.28	0.52
G40-800/5260 [72]	173	10	10	6.94	0.33	0.33	0.49
Western Hemlock[106]	10,100	313	586	323	0.485	0.423	0.382
Douglas-fir [106]	13,600	680	925	870	0.449	0.292	0.374
Ponderosa-Pine[106]	9.5	0.788	1.159	1.311	0.4	0.337	0.359

Table 2

Damage factor $\rho = \frac{K_{Ic}^2}{K_{IIc}^2}$ for various wooden materials.

Criteria	ρ	Norway Spruce	Red Spruce	Scot Pine
Romanowicz [48]	$\frac{c_{RL}}{c_R}$	0.1456	0.0368	0.1378
GSED [44]	$\frac{A_{22}(\varphi)}{A_{11}(\varphi)}$	0.0517	0.0523	0.055
SER_J [39]	$\frac{E_I}{E_{II}}$	0.2616	0.2778	0.2598
SED_J [39]	$\frac{c_{66}g_{12}^2(0)}{c_{11}f_{11}^2(0)+c_{22}f_{22}^2(0)+2c_{12}f_{11}(0)g_{11}(0)}$	0.7138	0.6827	0.3601
MPS_J [39]	$\frac{1}{f_{11}(0)}$	0.0684	0.0772	0.0675
MSS [91]	$(\frac{2}{f_{11}(0)-f_{22}(0)})^2$	0.5018	0.5918	0.4927
strength approach [50]	$2[(\frac{T_m}{T_M})+(\frac{T_m}{T_M})^2]$	0.175	0.0582	0.1551
micro_RIS [49]	$\frac{(5-\nu)(\xi\sqrt{\lambda}+\nu_{LR}\lambda)^2}{(10-3\nu)(1+0.5\nu_{LR}(1+\lambda))^2}$	0.0581	0.0531	0.0128
SED [75]	$\frac{c_{66}}{\xi_3^2(\frac{c_{11}}{\xi_1^2}+\frac{c_{22}}{\xi_2^2}+2\frac{c_{12}}{\xi_1\xi_2})}$	0.0572	0.0668	0.4884

Table 3

Damage factor $\rho = \frac{K_{Ic}^2}{K_{IIc}^2}$ for various wooden materials.

Criteria	ρ	Western Hemlock	Ponderosa-Pine	Douglas-fir
Romanowicz [48]	$\frac{c_{RL}}{c_R}$	0.0609	0.0364	0.0561
r_GSED [44]	$\frac{A_{22}(\varphi)}{A_{11}(\varphi)}$	0.0485	0.0554	0.0434
SER_J [39]	$\frac{E_I}{E_{II}}$	0.176	0.3493	0.2608
SED_J [39]	$\frac{c_{66}g_{12}^2(0)}{c_{11}f_{11}^2(0)+c_{22}f_{22}^2(0)+2c_{12}f_{11}(0)g_{11}(0)}$	0.5235	0.501	0.5754
MPS_J [39]	$\frac{1}{f_{11}(0)}$	0.031	0.122	0.068
MSS [91]	$(\frac{2}{f_{11}(0)-f_{22}(0)})^2$	0.1826	1.1525	0.4979
strength approach [50]	$2[(\frac{T_m}{T_M})+(\frac{T_m}{T_M})^2]$	0.0527	0.0423	0.0514
micro_RIS [49]	$\frac{(5-\nu)(\xi\sqrt{\lambda}+\nu_{LR}\lambda)^2}{(10-3\nu)(1+0.5\nu_{LR}(1+\lambda))^2}$	0.032	0.0283	0.0437
SED [75]	$\frac{c_{66}}{\xi_3^2(\frac{c_{11}}{\xi_1^2}+\frac{c_{22}}{\xi_2^2}+2\frac{c_{12}}{\xi_1\xi_2})}$	0.0105	0.1022	0.0419

$$S_c = A_{11}(\theta)K_I^2 + 2A_{12}(\theta)K_IK_{II} + A_{22}(\theta)K_{II}^2 + A_{13}(\theta)K_I + A_{23}(\theta)K_{II} + A_{33} \tag{24}$$

In which, A_{ij} are defined as:

$$A_{11} = \frac{1}{4\pi}\left(\frac{C_{11}}{\xi_1^2}f_{11}^2 + \frac{C_{22}}{\xi_2^2}f_{22}^2 + \frac{C_{66}}{\xi_3^2}f_{12}^2 + 2\frac{C_{12}}{\xi_1\xi_2}f_{11}f_{22}\right) \tag{25}$$

$$A_{12} = \frac{1}{4\pi}\left(\frac{C_{11}}{\xi_1^2}f_{11}g_{11} + \frac{C_{22}}{\xi_2^2}f_{22}g_{22} + \frac{C_{66}}{\xi_3^2}f_{12}g_{12} + \frac{C_{12}}{\xi_1\xi_2}(f_{11}g_{22}+f_{22}g_{11})\right) \tag{26}$$

$$A_{22} = \frac{1}{4\pi}\left(\frac{C_{11}}{\xi_1^2}g_{11}^2 + \frac{C_{22}}{\xi_2^2}g_{22}^2 + \frac{C_{66}}{\xi_3^2}g_{12}^2 + 2\frac{C_{12}}{\xi_1\xi_2}g_{11}g_{22}\right) \tag{27}$$

$$A_{13} = T\sqrt{\frac{r}{2\pi}}\left(\frac{C_{11}}{\xi_1^2}f_{11} + \frac{C_{16}}{\xi_1\xi_3}f_{12} + \frac{C_{12}}{\xi_1\xi_2}f_{22}\right) \tag{28}$$

$$A_{23} = T\sqrt{\frac{r}{2\pi}}\left(\frac{C_{11}}{\xi_1^2}g_{11} + \frac{C_{16}}{\xi_1\xi_3}g_{12} + \frac{C_{12}}{\xi_1\xi_2}g_{22}\right) \tag{29}$$

$$A_{33} = \frac{rC_{11}}{2\xi_1^2}T^2 \tag{30}$$

InA_{i3}, the distance from the crack tip is put in the criterion, which is defined for the isotropic material using SED criterion [94]:

$$r_c = \frac{(1+\nu_m)(5-8\nu_m)}{4\pi}\left(\frac{K_{Ic}}{\sigma_c}\right)^2 \tag{31}$$

In this equation,ν_m,σ_c, and K_{Ic} are the Poisson's ratio, strength, and pure mode I toughness of the isotropic solid materials.

Eq. (24) is the general form of the ESED criterion that considers the *T*-stress term. This criterion, however, fails to include the physical procedure of the fracture. Since it only considers the stress state at the crack tip. In composite materials, FPZ is created at the crack tip that causes the nonlinear fracture behavior of the material and dissipates the considerable amount of energy that is subjected to the material. Eq. (24) excludes FPZ, consequently, excludes the important part of energy dissipated at the crack tip and cannot precisely predict the fracture behavior of the material. In the next section, a novel suggested idea is thoroughly explained, which brings the effect of FPZ in Eq. (24).

4. Development of ISEDM criterion with the midpoint

The RIS concept is vigorously elucidated and regards the true failure process in composite materials. A couple of fracture criteria are derived

based on this concept. However, they fail to perfectly encompass the physics of the fracture procedure. One must notice that at the crack tip of the quasi-brittle materials, a FPZ is created that noticeably dissipates the energy. In this FPZ, the material at the crack tip commences to non-linearly behavior induced by some phenomena such as fiber bridging, micro-cracking, and plastic transformation of the material that toughen the material at the crack tip. These mechanisms absorb the energy of the loaded structure, which prevents catastrophic failure and delays crack growth [57,58,95]. Substantial as the FPZ is in the fracture phenomenon, it was disregarded in the primary mixed-mode loading criteria. Gradually, the effect of FPZ crawls into the research [48] so it is recently displayed that considering the effect of FPZ in the fracture process remarkably improves the accuracy of the failure prediction [55,96]. Therefore, it is of great importance to regard the FPZ in the fracture study. In pure mode I, the size of the FPZ is trivially small. With the emergence of pure mode II and the passage of pure mode I, the size of FPZ becomes larger. Consequently, as the size of the FPZ grows, the effect of the FPZ at the fracture procedure increases. Please note that the size of FPZ at pure mode II is significant and much larger than the size of FPZ at pure mode I. The larger the size of the FPZ is, the tougher the material is since more energy is required to create FPZ [93,97,98]. On one hand, the available mixed-mode fracture criteria predict the crack growth based on the mode I critical stress intensity factor, which is derived using various methods. These fracture criteria overlooked the effect of FPZ when mode II is dominant. Therefore, it is rational to reconsider these criteria and derive the fracture criteria based on the mode II critical stress intensity factor. However, the arduous experimental conditions to simulate the pure mode II prevents scholars to derive fracture criteria based on the value ofK_{IIc}. In addition, fracture criteria based on merely mode II, overestimate the fracture behavior of material when mode I is dominant. Hence, it is concluded that a precise mixed-mode fracture criterion has to exploit an equivalent stress intensity factor that equally includes the effect of the creation of FPZ, and subsequently, toughening the materials at mode I and II.

To develop this novel criterion, one may take into account the energy dissipated for the creation of the FPZ by employing the experimental data of the orthotropic material in the midpoint, where the nonlinear behavior of the material is more considerable. The midpoint of experimental data in mixed-mode I/II loading is employed and can be extracted by conducting the commonplace tension test, which follows the defined standard for obtaining the fracture toughness for anisotropic materials.

In Ref [99], a new approach to develop the prediction of fracture in orthotropic materials was proposed as the midpoint of experimental data. The midpoint of experimental data is determined after testing and examining mode I and II SIF's.In the experimental test of specimens, different mode mixities from pure mode I to pure mode II are possible. The midpoint of experimental data is the point at which K_I and K_{II} are very close to each other. This point corresponds to mid-level mode mixity. Considering the effect of *T*-stress, the SED criterion is restated as follows:

$$S_c = A_{11}(\theta)K_I^2 + 2A_{12}(\theta)K_IK_{II} + A_{22}(\theta)K_{II}^2 + A_{13}(\theta)K_I + A_{23}(\theta)K_{II} + A_{33} \tag{32}$$

According to the strain energy density criterion, fracture occurs when the strain energy density reaches a critical value. The critical value is the same in each loading mode. Mode I and II are inherently related. So, a physics-based relationship between different loading modes can be extracted. For each experimental data which is equivalent to a fracture point in mixed-mode I / II loading, critical strain energy density is constant. So the following relationship is established:

$$S_{I_c} = S_{II_c} = S_{I/II_c} \tag{33}$$

The outputs of the test are (K_{Im},K_{IIm}), which are the critical toughness of the material at the midpoint. For pure mode I and a mid-point in mixed-mode I / II loading, strain energy density are as follows:

$$S_{I_c} = A_{11}(\theta_{Ic})K_{Ic}^2 + A_{13}(\theta_{Ic})K_{Ic} + A_{33} \tag{34}$$

$$S_{I/II_c} = A_{11}(\theta_M)K_{I_M}^2 + 2A_{12}(\theta_M)K_{I_M}K_{II_M} + A_{22}(\theta_M)K_{II_M}^2 + A_{13}(\theta_M)K_{I_M} + A_{23}(\theta_M)K_{II_M} + A_{33} \tag{35}$$

Finally, mode I fracture toughness can be extracted as follows:

$$K_{Ic} = \frac{-A_{13}(\theta_{Ic}) + \sqrt{A_{13}(\theta)^2 + 4A_{11}(\theta_{Ic}).[A_{11}(\theta_M)K_{I_M}^2 + 2A_{12}(\theta_M)K_{I_M}K_{II_M} + A_{22}(\theta_M)K_{II_M}^2 + A_{13}(\theta_M)K_{I_M} + A_{23}(\theta_M)K_{II_M}]}}{2A_{11}(\theta_{Ic})} \tag{36}$$

The general form of stress or energy fracture criteria for orthotropic materials is as follows:

$$K_I^2 + \rho K_{II}^2 = K_{Ic}^2 \tag{37}$$

The general form of the orthotropic material fracture equation and the damage factor using midpoint (K_{Im}, K_{IIm}) is as follows:

$$K_I^2 + \rho_M(K_{II}^2 - K_{II_M}^2) = K_{I_M}^2 \tag{38}$$

In which:

$$\rho_M = \frac{K_{Ic}^2 - K_{I_M}^2}{K_{II_M}^2} \tag{39}$$

In this way, the damage factor of the Improved Strain Energy Density criterion with Mid-point (ISEDM) is extracted as follows:

$$\rho_M = \left[\frac{-A_{13}(\theta_{Ic}) + \sqrt{A_{13}(\theta_{Ic})^2 + 4A_{11}(\theta_{Ic}).[A_{11}(\theta_M)K_{I_M}^2 + 2A_{12}(\theta_M)K_{I_M}K_{II_M} + A_{22}(\theta_M)K_{II_M}^2 + A_{13}(\theta_M)K_{I_M} + A_{23}(\theta_M)K_{II_M}]}}{2A_{11}(\theta_{Ic})K_{II_M}^2}\right]^2 - \frac{K_{I_M}^2}{K_{II_M}^2} \tag{40}$$

Thus ISEDM as a novel fracture criterion is developed. Damage factor depends only on the SIF's of midpoint (K_{I_M}, K_{II_M}) and crack initiation angles at the midpoint and pure mode I.

5. Crack initiation angle

Based on the ISEDM criterion, the crack will grow in a direction where $S(\theta)$ is minimum [86]. In this case, we have:

$$\frac{\partial S(\theta)}{\partial \theta} = 0 \tag{41}$$

$$\frac{\partial^2 S(\theta)}{\partial \theta^2} > 0 \tag{42}$$

In the absence of the *T*-stress term, the following relationship is established:

$$\frac{\partial S(\theta)}{\partial \theta} = \frac{\partial A_{11}(\theta)}{\partial \theta} K_I^2 + 2\frac{\partial A_{12}(\theta)}{\partial \theta} K_I K_{II} + \frac{\partial A_{22}(\theta)}{\partial \theta} K_{II}^2 \tag{43}$$

In which,A_{ij} coefficient is derived as follows:

$$\frac{\partial A_{11}(\theta)}{\partial \theta} = \frac{1}{2\pi}\left(\frac{C_{11}}{\xi_1^2} f_{11}\frac{\partial f_{11}}{\partial \theta} + \frac{C_{22}}{\xi_2^2} f_{22}\frac{\partial f_{22}}{\partial \theta} + \frac{C_{12}}{\xi_1 \xi_2}\left[f_{11}\frac{\partial f_{22}}{\partial \theta} + f_{22}\frac{\partial f_{11}}{\partial \theta}\right]\right) \tag{44}$$

$$\begin{aligned}\frac{\partial A_{12}(\theta)}{\partial \theta} = \frac{1}{4\pi}\Bigg(&\frac{C_{11}}{\xi_1^2}\left[f_{11}\frac{\partial g_{11}}{\partial \theta} + g_{11}\frac{\partial f_{11}}{\partial \theta}\right] + \frac{C_{22}}{\xi_2^2}\left[f_{22}\frac{\partial g_{22}}{\partial \theta} + g_{22}\frac{\partial f_{22}}{\partial \theta}\right] + \\ &\frac{C_{66}}{\xi_3^2}\left[f_{12}\frac{\partial g_{12}}{\partial \theta} + g_{12}\frac{\partial f_{12}}{\partial \theta}\right] + \frac{C_{12}}{\xi_1 \xi_2}\left[f_{11}\frac{\partial g_{22}}{\partial \theta} + g_{22}\frac{\partial f_{11}}{\partial \theta} + f_{22}\frac{\partial g_{11}}{\partial \theta} + g_{11}\frac{\partial f_{22}}{\partial \theta}\right]\end{aligned} \tag{45}$$

$$\frac{\partial A_{22}(\theta)}{\partial \theta} = \frac{1}{2\pi}\left(\frac{C_{11}}{\xi_1^2} g_{11}\frac{\partial g_{11}}{\partial \theta} + \frac{C_{22}}{\xi_2^2} g_{22}\frac{\partial g_{22}}{\partial \theta} + \frac{C_{12}}{\xi_1 \xi_2}\left[g_{11}\frac{\partial g_{22}}{\partial \theta} + g_{22}\frac{\partial g_{11}}{\partial \theta}\right]\right) \tag{46}$$

In pure mode I and II, crack initiation angles θ_{Ic} and θ_{IIc} are extracted as follows [86]:

$$\frac{\partial S(\theta)}{\partial \theta} = \frac{\partial A_{11}(\theta)}{\partial \theta} K_{Ic}^2 = 0 \rightarrow \frac{\partial A_{11}(\theta)}{\partial \theta} = 0 \tag{47}$$

$$\frac{\partial S(\theta)}{\partial \theta} = \frac{\partial A_{22}(\theta)}{\partial \theta} K_{IIc}^2 = 0 \rightarrow \frac{\partial A_{22}(\theta)}{\partial \theta} = 0 \tag{48}$$

These equations have two roots and one of them can be satisfied in Eq (42). By numerical solutions of Eq`s (47) and (48), θ_{Ic} and θ_{IIc} is derived. These angles for any material properties are extracted.

6. Estimation of strain energy release rate with ISEDM criterion

Both stress intensity factor,*K*, and strain energy release rate,*G*, are employed to predict the strength of a structure; however, they are derived by completely different methods and their dimensions are distinct. For engineering purposes and compliance with standards, the measurement of *K* and *G* is important. The strain energy release rate is developed based on the balance of total energy, or equilibrium equations [100], and the stress intensity factor is developed based on the stress state at the crack tip [101]. Since both of these quantities, *K* and *G* are employed to anticipate the fracture behavior of materials, they must be pertinent to each other. Strain energy release rate has a global nature and defines as required energy for the creation of the crack surface.*G*, therefore, encompasses the whole damage mechanism of the structure. Nonetheless,*K* highly depends on the stress distribution in the vicinity of the crack tip and is intensely sensitive to the geometry of the crack tip. Therefore, *K* only includes the effects of the cohesion of the material at the crack tip. Having well recognized the crack tip vicinity and geometry, the value of the stress intensity factor is effortlessly obtained. The relation between *K* and *G* has always been regarded. Not only does it benefit to derive the value of the K_{IIc} based on the well-defined experimental survey, but it also assists to evaluate the accuracy of the criteria based on toughness.

A number of researches have revealed the relationship between *G* and *K* [40,49,73–77]. However, a considerable discrepancy between them is not well illuminated. A relationship between the ratio of strain energy release rate of pure mode I and II, which is obtained through experimental test, and the ratio of stress intensity factor for pure mode I and II, which is formulated based on the SED criterion for anisotropic material, are derived [72]. First, Amaral and Alderliesten [72] restated that being independent of the loading mode, strain energy density controls the brittle fracture of isotropic materials. The ratio of pure mode I and II for sample rocks have a good agreement with the experimental result of this ratio. Given the anisotropic stress state, the researchers employed a relation between the SED and strain energy release rate to earn the $(G_{IIc})_{SED}$ which means that G_{IIc} is theoretically derived from the SED for orthotropic materials. They declared that the strain energy release rate for pure mode I and II is not the same in anisotropic materials, since several damage mechanisms in pure mode II around the crack tips occur and cause the overestimation of strain energy release rate for pure mode II. Moreover, despite the value ofG_{Ic}, the value of G_{IIc} that is obtained by the experimental data does not indicate the initiation of the damage, on the ground that there are a couple of damage mechanisms ahead of the crack tip that toughens the material before the crack growth [72].

For three composite materials, they displayed that the value of reported experimental G_{IIc} conducted by end-notch flexure specimens (ENF) test [102,103] is much more than the reported$(G_{IIc})_{SED}$, the percentage of the $\frac{(G_{IIc})_{SED}}{(G_{IIc})_{ENF}}$ is about 0.25. Carefully considering the equations of strain energy release rate, $G_{Ic} = F_I K_{Ic}^2$ and$G_{IIc} = F_{II} K_{IIc}^2$, it is clear-cut that the value of the $(G_{IIc})_{SED}$ depends on the value of the stress intensity factor in pure mode I and II. To decrease the discrepancy between $(G_{IIc})_{SED}$ and$(G_{IIc})_{ENF}$, the precise stress intensity factor which includes the effect of damage mechanisms at the far distance, ahead of the crack tip, is required. Therefore, it is necessary to consider more precise the physics-based fracture phenomena. The ESED and ISEDM criteria are based on RIS, Eqs. (23) and (40), is applied for the materials of [102]. The critical stress intensity factors, K_{Ic} and K_{IIc} are obtained based on ESED and ISEDM and replaced in the equations of strain energy release rate for pure mode I and II. Therefore, $(G_{IIc})_{ESED}$ and $(G_{IIc})_{ISEDM}$ are obtained based on the following formula:

$$(G_{IIc})_{ESED} = G_{Ic}.\frac{F_{II}}{F_I}.\frac{A_{11}(0)}{A_{22}(\theta_c)} \tag{49}$$

$$(G_{IIc})_{ISEDM} = G_{Ic}.\frac{F_{II}}{F_I}.\frac{K_{II_M}^2}{\left[\frac{-A_{13}(\theta_{Ic}) + \sqrt{A_{13}(\theta_{Ic})^2 + 4A_{11}(\theta_{Ic}).\left[A_{11}(\theta_M)K_{I_M}^2 + 2A_{12}(\theta_M)K_{I_M}K_{II_M} + A_{22}(\theta_M)K_{II_M}^2 + A_{13}(\theta_M)K_{I_M} + A_{23}(\theta_M)K_{II_M}\right]}}{2A_{11}(\theta_{Ic})}\right]^2 - K_{I_M}^2} \tag{50}$$

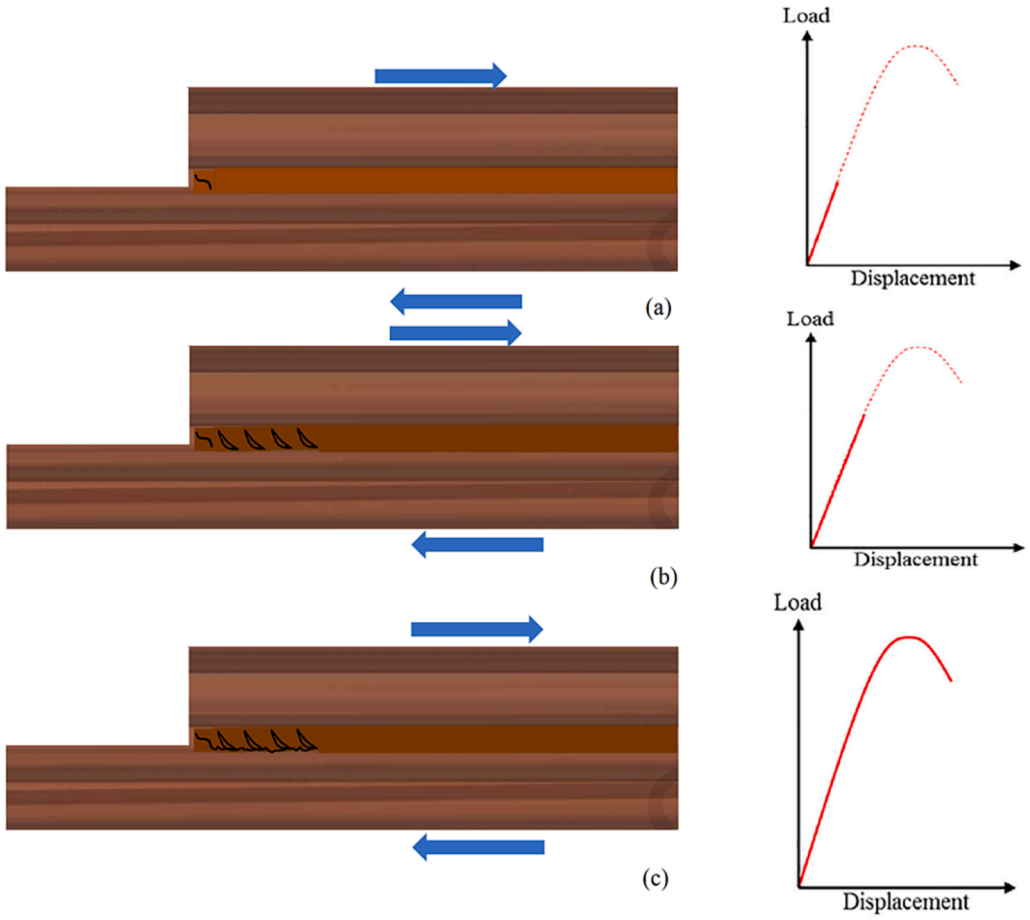

Fig. 2. Fracture process based on micromechanical approach under pure mode II condition. (a) first microcrack phase (b) cusp formation phase (c) coalescence phase [72].

Table 4
Calculated SERR for three composite materials.

Composite materials	$G_{Ic}(J/m^2)$[104]	$(G_{IIc})_{ENF}(J/m^2)$[104]	$(G_{IIc})_{SED}(J/m^2)$[72]	$(G_{IIc})_{ESED}(J/m^2)$	$(G_{IIc})_{ISEDM}(J/m^2)$
IM7/8552	200	800	195	632.21	769
G40-800/5260	240	900	237	839.31	873
AS4/3501–6	220	650	216	848.31	621

Table 5
Ratio between predicted SERR based on fracture criterion to the experiment value of SERR for three composite materials.

Composite materials	$\frac{(G_{IIc})_{SED}}{(G_{IIc})_{ENF}}$[72]	$\frac{(G_{IIc})_{ESED}}{(G_{IIc})_{ENF}}$	$\frac{(G_{IIc})_{ISEDM}}{(G_{IIc})_{ENF}}$
IM7/8552	0.24	0.79	0.96
G40-800/5260	0.26	0.93	0.97
AS4/3501–6	0.33	1.3	0.95

In which F_I and F_{II} are equation based on the angular function of the stress state of the anisotropic materials [80].

$$F_I = \sqrt{\frac{C_{11}C_{22}}{2}}\left[\sqrt{\frac{C_{22}}{C_{11}}} + \frac{2C_{12}+C_{66}}{2C_{11}}\right]^{\frac{1}{2}} \tag{51}$$

$$F_{II} = \sqrt{\frac{C_{11}^2}{2}}\left[\sqrt{\frac{C_{22}}{C_{11}}} + \frac{2C_{12}+C_{66}}{2C_{11}}\right]^{\frac{1}{2}} \tag{52}$$

Therefore, considering the extracted value of G_{Ic} and ESED and ISEDM criteria, Eqs. (23) and (40), the value of G_{IIc} can be estimated.

Damage mechanisms that act during fracture are a main part of the crack growth process. Changes in damage mechanisms lead to changes in dissipated energy in crack growth. So, to describe the dissipated energy in the fracture process, in addition to SIF's, one needs a complete stress distribution function. The description and distribution of stress are done through the SED function.

As shown in Fig. 2 for HTA/6376C carbon/epoxy under end notched flexure (ENF) test as reported in Ref [72], the first crack growth occurs when the load is still less than the critical load and load drop is not observed. The first crack growth cannot be seen with the naked eye. As the load increases, cusps form. As the load increases again, the micro-cracks merge and then a load drop is observed. So the onset of fracture occurs before the specimen reach G_{IIc} [72].

The important point is that G_{Ic} is related to the onset of crack growth in mode I and is obtained experimentally, while G_{IIc} is related to when the micro-cracks form coalescence in the front of the crack tip and is obtained through experimental testing.

According to theG_{Ic}, Eq. (49) and (50), the value $(G_{IIc})_{ESED}$ and $(G_{IIc})_{ISEDM}$ for the composite materials [104] are calculated in Table 4

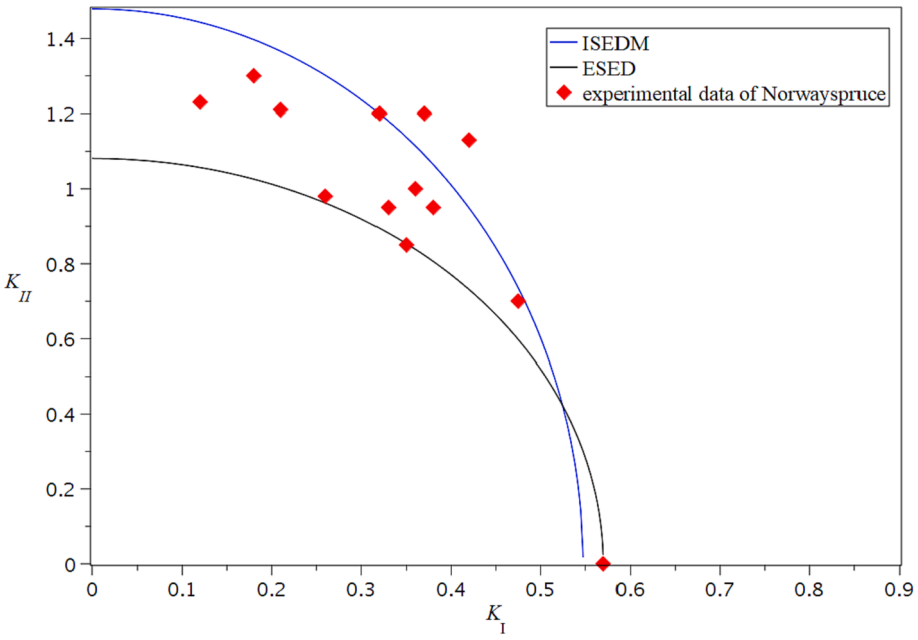

Fig. 3. FLC's of ISEDM and ESED criteria in comparison with Norway-spruce experimental data [38].

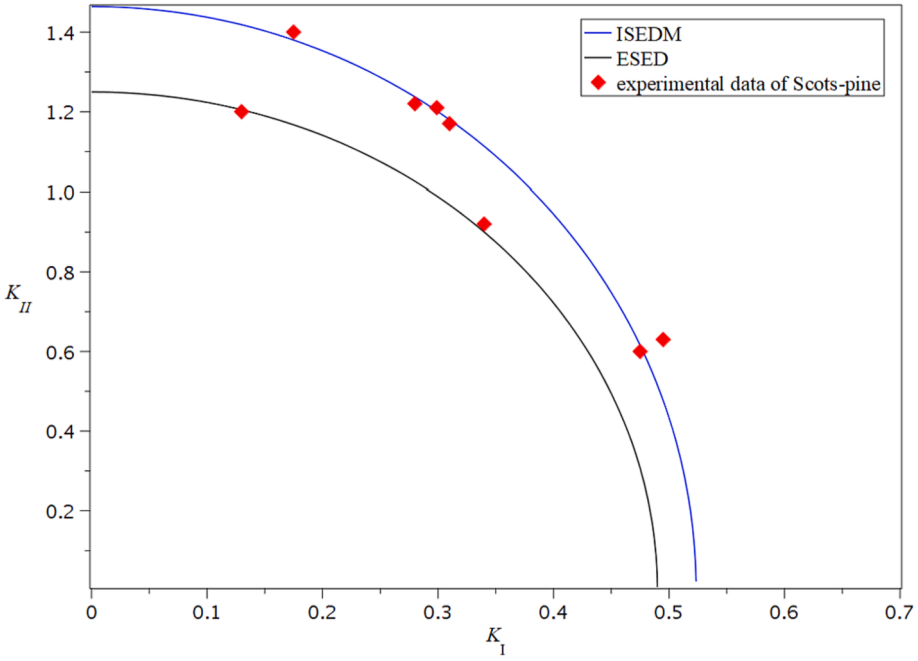

Fig. 4. FLC's of ISEDM and ESED criteria in comparison with Scots-pine experimental data [39].

and 5.

Table 5 indicates that the value of SERR for pure mode II for three materials is improved using RIS. In Table 3, the ratio of $\frac{(G_{IIc})_{ISEDM}}{(G_{IIc})_{ENF}}$ is almost 96 %, which is a satisfying prediction compared to the previous work [72]. $\frac{(G_{IIc})_{ISEDM}}{(G_{IIc})_{ENF}}$ depends on the micro-cracks density in the fracture process zone and the properties of the composite material. As it is observed, the prediction for composite materials is reasonable. In Table 5, the ISEDM criterion can provide a more accurate estimation forG_{IIc}. In explaining the compatibility of the ISEDM criterion with the experimental results, it is stated that the effects of the FPZ are considered using the midpoint of experimental data. In addition, the RIS model is an acceptable model for predicting the fracture behavior of orthotropic materials. In the RIS theory, the ReSt coefficients are employed, which are valid and reliable for highly orthotropic materials with unidirectionally aligned fibers. Generally, for different materials and employed criteria, it is demonstrated that the RIS concept is more compatible than the LEFM theory. Therefore, the importance of the RIS concept is clear and it ought to be involved in the study of fracture response of composite material. Also, it is expected that regarding *T*-stress in the calculations of RIS theory positively affects the anticipation of the$(G_{IIc})_{SED}$.

7. Results and discussion

The SED criterion is modified based on the midpoint stress intensity factor derived based on the mixed-mode test. In addition, the fracture

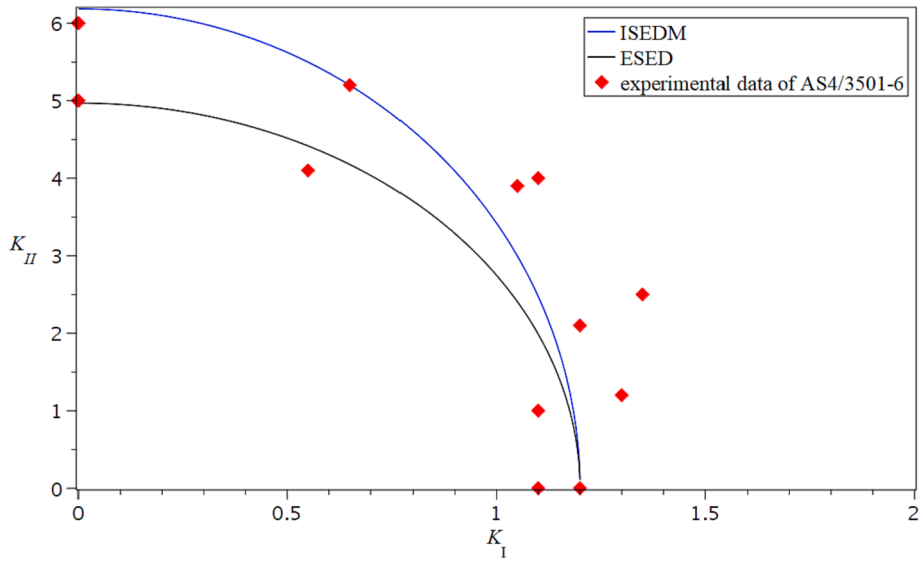

Fig. 5. FLC's of ISEDM and ESED criteria in comparison with AS4/3501–6 experimental data [105].

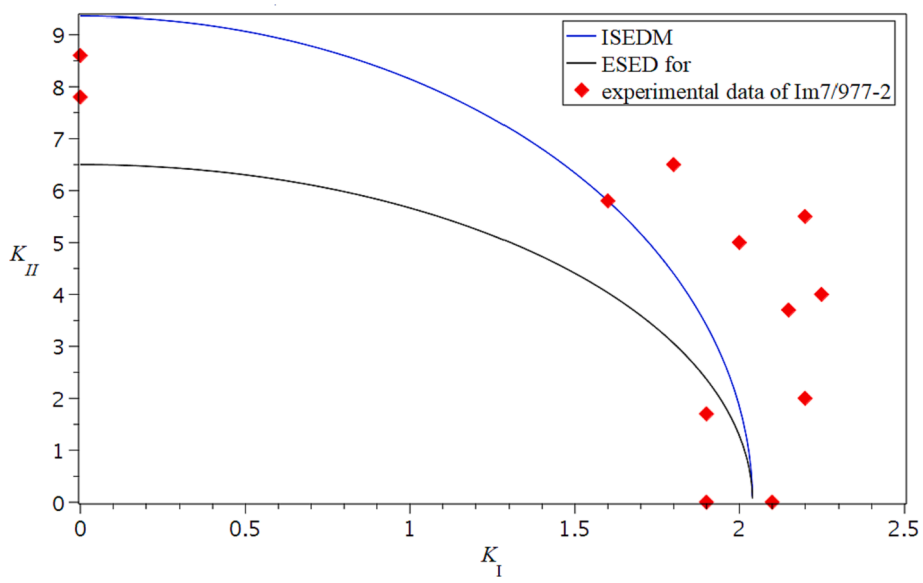

Fig. 6. FLC's of ISEDM and ESED criteria in comparison with IM7/977–2 experimental data [105].

Table 6
Required parameters to investigate the fracture of the composite materials (GPa).

Composite material	θ_{Ic}	θ_{IIc}	θ_M	K_{I_M}	K_{II_M}
Scots-Pine	44.7	76.7	55.5	0.31	1.2
Norway-Spruce	34.2	79.1	56.5	0.32	1.22
Im7/977–2	36.9	80.4	58	1.6	5.8
AS4/3501–6	41.8	80.2	60	0.65	5.2

limit curve of orthotropic materials is extracted using strain energy density criterion and midpoint. Finally, the validity of the proposed criterion is evaluated by comparing fracture limit curves with experimental data.

Figs. 3-6 depict the fracture behavior of unidirectional laminated composites such as Im7/977–2 and AS4/3501–6 and wood specimens such as Norway-Spruce and Scots-Pine under mixed-mode I / II loading pertinent to ISEDM. FLC's are compared with the experimental data available in the references [38,39,105]. Tables 6 reports required parameters to extract the fracture behavior of materials, respectively. K_{I_M} and K_{II_M} are the midpoint of experimental data in Ref [38,39,105].

Based on the ISEDM approach, crack deviates in the direction that strain energy density reaches its minimum value. Thus, crack initiation angles are extracted for these materials and they are very close to these angles in reference [55]. The important point is related to the crack initiation angle in the midpoint, the exact value of this angle has an important effect on the prediction of fracture behavior for orthotropic materials. Crack initiation angle in midpoint is considered the average of crack initiation angles in pure mode I and II. The value of this angle is obtained with:

$$\theta_M = \frac{\theta_{Ic} + \theta_{IIc}}{2} \tag{53}$$

Another important point in this section is that the fracture limit curve depends on the midpoint in experimental data. Some experimental data are lower or higher than the overall orthotropic fracture behavior. For this reason, the relevant fracture limit curve may predict K_{Ic} slightly more or less than the value of this coefficient in the references.

Establishing experimental conditions to extract K_{IIc} is very difficult. Therefore, different values of K_{IIc} have been reported in different references. By setting the test conditions in mixed-mode without performing the test in pure mode II, this criterion can be well estimatedK_{IIc}. So, this criterion is efficient for predicting the fracture behavior of orthotropic materials.

The main improvements in evaluating the fracture behavior of orthotropic materials by ISEDM criterion are:

1) Employing RIS concept to modeling orthotropic materials
2) Base on a precise physics-based assumption, crack initiates along minimum strain energy density for the mid-point of experimental data.
3) Changing fracture point from pure mode I to mid-point base on minimum strain energy density causes the effects of FPZ to be considered.

8. Conclusion

ISEDM as a new criterion for mixed-mode loading in accordance with SED is proposed to predict the fracture response. Correctly considering the physical phenomenon of the fracture, this criterion relates the microscopic damage of the matrix to the macroscopic failure of composite materials. The physical phenomena that involve in the fracture find a place in the criterion using three items: RIS, *T*-stress, and FPZ.

It is observed that the crack initiates and propagates in the matrix reinforced fibers. The isotropic stress state is replaced with the anisotropic stress state in the vicinity of the crack tip based on the RIS theory. The crack growth is assumed along minimum strain energy density, and crack initiation angle in pure mode I and II at microscopic scale are extracted. Crack initiation angle in mid-point is considered the average of crack initiation angles in pure mode I and II. The effect of the creation of FPZ at dissipating the energy of the loaded structure and toughening the material, which is more noticeable when mode II is dominant, is regarded using the strain energy density of a mixed-mode loading. To equally include the effects of mode I and II at the formation of the FPZ, the mid-point in experimental data is considered. The *T*-stress term, which directly affects FPZ and causes the emergence of the damage mechanisms around the crack tip, particularly, when mode II is dominant is regarded. This macroscopic fracture criterion finely encompasses the micromechanical damage and precisely predicts the fracture behavior.

The main reasons for improving the fracture behavior of orthotropic materials based on the proposed criterion are as follows:

1) Applying the RIS concept to model orthotropic materials, which is perfectly consistent with the nature of the failure in these materials, is one of the important reasons for improving the prediction of fracture behavior.
2) An important innovation of this criterion is to consider the effects of the FPZ using the midpoint of the experimental data without calculating the energy dissipation in this zone.

Comparing the FLC's of ISEDM criterion with the experimental data proves the superiority of the proposed criterion and indicates that using midpoint as a fracture point instead of pure mode I point is an important step in accurately evaluating the fracture behavior of orthotropic materials.

CRediT authorship contribution statement

Zahra Khaji: Software, Validation, Formal analysis, Data curation, Writing – original draft. **Mahdi Fakoor:** Conceptualization, Methodology, Investigation, Supervision, Writing – review & editing. **Hannaneh Manafi Farid:** Software, Formal analysis, Data curation, Writing – original draft. **René Alderliesten:** Conceptualization, Methodology, Investigation, Writing – review & editing.

Declaration of Competing Interest

The authors declare that they have no known competing financial interests or personal relationships that could have appeared to influence the work reported in this paper.

Appendix A

$f_{ij}(\theta)$ and $g_{ij}(\theta)$ coefficients in Eqs. (7)–(9) are defined as follows:

$$f_{11}(\theta) = \cos\frac{\theta}{2}\left(1 - \sin\frac{\theta}{2}\sin\frac{3\theta}{2}\right) \tag{A1}$$

$$f_{22}(\theta) = \cos\frac{\theta}{2}\left(1 + \sin\frac{\theta}{2}\sin\frac{3\theta}{2}\right) \tag{A2}$$

$$f_{12}(\theta) = \sin\frac{\theta}{2}\cos\frac{\theta}{2}\cos\frac{3\theta}{2} \tag{A3}$$

$$g_{11}(\theta) = -\sin\frac{\theta}{2}\left(2 + \cos\frac{\theta}{2}\cos\frac{3\theta}{2}\right) \tag{A4}$$

$$g_{22}(\theta) = \sin\frac{\theta}{2}\cos\frac{\theta}{2}\cos\frac{3\theta}{2} \tag{A5}$$

$$g_{12}(\theta) = \cos\frac{\theta}{2}\left(1 - \sin\frac{\theta}{2}\sin\frac{3\theta}{2}\right) \tag{A6}$$

References

[1] G.L. Golewski, On the special construction and materials conditions reducing the negative impact of vibrations on concrete structures, Mater. Today:. Proc. 45 (2021) 4344–4348.
[2] P. Jakubczak, J. Bieniaś, K. Dadej, Experimental and numerical investigation into the impact resistance of aluminium carbon laminates, Compos. Struct. 244 (2020), 112319.
[3] V.V. Vasiliev, E.V. Morozov, Advanced mechanics of composite materials and structural elements, Newnes, 2013.
[4] M. Marjanović, G. Meschke, D. Vuksanović, A finite element model for propagating delamination in laminated composite plates based on the Virtual Crack Closure method, Compos. Struct. 150 (2016) 8–19.
[5] C.h. Hochard, S.t. Miot, Y. Thollon, Fatigue of laminated composite structures with stress concentrations, Compos. B Eng. 65 (2014) 11–16.
[6] A. Tabiei, W. Zhang, Composite laminate delamination simulation and experiment: A review of recent development, Appl. Mech. Rev. 70 (3) (2018), 030801.
[7] G. Guillamet, A. Turon, J. Costa, P. Linde, A quick procedure to predict free-edge delamination in thin-ply laminates under tension, Eng. Fract. Mech. 168 (2016) 28–39.
[8] P.A. Carraro, E. Novello, M. Quaresimin, M. Zappalorto, Delamination onset in symmetric cross-ply laminates under static loads: Theory, numerics and experiments, Compos. Struct. 176 (2017) 420–432.
[9] A. Wagih, et al., Damage sequence in thin-ply composite laminates under out-of-plane loading, Compos. A Appl. Sci. Manuf. 87 (2016) 66–77.
[10] G.L. Golewski, Physical characteristics of concrete, essential in design of fracture-resistant, dynamically loaded reinforced concrete structures, Material Design & Processing Communications 1 (5) (2019), e82.
[11] H. Masaki, O. Shojiro, C.-G. Gustafson, T. Keisuke, Effect of matrix resin on delamination fatigue crack growth in CFRP laminates, Eng. Fract. Mech. 49 (1) (1994) 35–47.
[12] C. Harvey, M.R. Eplett, S. Wang, Experimental assessment of mixed-mode partition theories for generally laminated composite beams, Compos. Struct. 124 (2015) 10–18.
[13] E. Wu, "Application of fracture mechanics to anisotropic plates," 1967.
[14] S. Mall, J.F. Murphy, J.E. Shottafer, Criterion for mixed mode fracture in wood, J. Eng. Mech. 109 (3) (1983) 680–690.
[15] J. R. Reeder, "A bilinear failure criterion for mixed-mode delamination," in *Eleventh Volume: Composite Materials—Testing and Design*: ASTM International, 1993.
[16] M. Kenane, M. Benzeggagh, Mixed-mode delamination fracture toughness of unidirectional glass/epoxy composites under fatigue loading, Compos. Sci. Technol. 57 (5) (1997) 597–605.
[17] E. Triki, B. Zouari, F. Dammak, Dependence of the interlaminar fracture toughness of E-Glass/Polyester woven fabric composites laminates on ply orientation, Eng. Fract. Mech. 159 (2016) 63–78.
[18] D. Gil and G. Golewski, "Effect of silica fume and siliceous fly ash addition on the fracture toughness of plain concrete in mode I," in *IOP Conference Series: Materials Science and Engineering*, 2018, vol. 416, no. 1: IOP Publishing, p. 012065.
[19] G. Golewski, "An analysis of fracture toughness in concrete with fly ash addition, considering all models of cracking," in *IOP Conference Series: Materials Science and Engineering*, 2018, vol. 416, no. 1: IOP Publishing, p. 012029.
[20] B. Szostak and G. Golewski, "Effect of nano admixture of CSH on selected strength parameters of concrete including fly ash," in *IOP Conference Series: Materials Science and Engineering*, 2018, vol. 416, no. 1: IOP Publishing, p. 012105.
[21] M. Aliha, M. Sarbijan, A. Bahmani, Fracture toughness determination of modified HMA mixtures with two novel disc shape configurations, Constr. Build. Mater. 155 (2017) 789–799.
[22] H. Rooholamini, A. Hassani, M. Aliha, Fracture properties of hybrid fibre-reinforced roller-compacted concrete in mode I with consideration of possible kinked crack, Constr. Build. Mater. 187 (2018) 248–256.
[23] G. Golewski, T. Sadowski, An analysis of shear fracture toughness KIIc and microstructure in concretes containing fly-ash, Constr. Build. Mater. 51 (2014) 207–214.
[24] G. Golewski, T. Sadowski, The fracture toughness the KIIIc of concretes with F fly ash (FA) additive, Constr. Build. Mater. 143 (2017) 444–454.
[25] S. Mehdinejad, H. Fazaeli, A. Moniri, A.S. Dabiri, Comparison of two criteria of stress intensity factor and fracture energy to investigate the behavior of asphalt mixtures under combined tensile-shear loading modes-A statistical approach, Constr. Build. Mater. 290 (2021), 123230.
[26] M. Ameri, A. Mansourian, S. Pirmohammad, M. Aliha, M. Ayatollahi, Mixed mode fracture resistance of asphalt concrete mixtures, Eng. Fract. Mech. 93 (2012) 153–167.
[27] A. Razmi, M. Mirsayar, On the mixed mode I/II fracture properties of jute fiber-reinforced concrete, Constr. Build. Mater. 148 (2017) 512–520.
[28] M. Aliha, A. Razmi, A. Mousavi, Fracture study of concrete composites with synthetic fibers additive under modes I and III using ENDB specimen, Constr. Build. Mater. 190 (2018) 612–622.
[29] A. Mansourian, S. Hashemi, M.R.M. Aliha, Evaluation of pure and mixed modes (I/III) fracture toughness of Portland cement concrete mixtures containing reclaimed asphalt pavement, Constr. Build. Mater. 178 (2018) 10–18.
[30] F. Yu, D. Sun, G. Sun, S. Ling, M. Hu, J. Ma, A modified mix design method for pervious concrete based on Mohr-Coulomb failure criterion, Constr. Build. Mater. 269 (2021), 121801.
[31] S. Yang, L. Li, Z. Sun, J. Wang, Q. Guo, Y. Yang, A closed-form fracture model to predict tensile strength and fracture toughness of alkali-activated slag and fly ash blended concrete made by sea sand and recycled coarse aggregate, Constr. Build. Mater. 300 (2021), 123976.
[32] X. Wan, C. Shen, P. Wang, T. Zhao, Y. Lu, A study on fracture toughness of ultra-high toughness geopolymer composites based on Double-K Criterion, Constr. Build. Mater. 251 (2020), 118851.
[33] V.E. Saouma, M.L. Ayari, D.A. Leavell, Mixed mode crack propagation in homogeneous anisotropic solids, Eng. Fract. Mech. 27 (2) (1987) 171–184.
[34] C. Carloni, L. Nobile, Maximum circumferential stress criterion applied to orthotropic materials, Fatigue Fract. Eng. Mater. Struct. 28 (9) (2005) 825–833.
[35] M. Hussain, S. Pu, and J. Underwood, "Strain energy release rate for a crack under combined mode I and mode II," in *Fracture analysis: Proceedings of the 1973 national symposium on fracture mechanics, part II*, 1974: ASTM International.
[36] L. Nobile, A. Piva, E. Viola, On the inclined crack problem in an orthotropic medium under biaxial loading, Eng. Fract. Mech. 71 (4–6) (2004) 529–546.
[37] E. Gdoutos, D. Zacharopoulos, E. Meletis, Mixed-mode crack growth in anisotropic media, Eng. Fract. Mech. 34 (2) (1989) 337–346.
[38] L.O. Jernkvist, Fracture of wood under mixed mode loading: II. Experimental investigation of Picea abies, Eng. Fract. Mech. 68 (5) (2001) 565–576.
[39] L.O. Jernkvist, Fracture of wood under mixed mode loading: I. Derivation of fracture criteria, Eng. Fract. Mech. 68 (5) (2001) 549–563.
[40] M. Fakoor, Augmented strain energy release rate (ASER): A novel approach for investigation of mixed-mode I/II fracture of composite materials, Eng. Fract. Mech. 179 (2017) 177–189.
[41] M. Fakoor, N.M. Khansari, General mixed mode I/II failure criterion for composite materials based on matrix fracture properties, Theor. Appl. Fract. Mech. 96 (2018) 428–442.
[42] M. Fakoor, R. Rafiee, S. Zare, Equivalent reinforcement isotropic model for fracture investigation of orthotropic materials, Steel and Composite Structures 30 (1) (2019) 1–12.
[43] Z. Khaji and M. Fakoor, "Strain Energy Release Rate in Combination with Reinforcement Isotropic Solid Model (SERIS): A new Mixed-mode I/II Criterion to Investigate Fracture Behavior of Orthotropic Materials," *Theoretical and Applied Fracture Mechanics*, p. 102962, 2021.
[44] H.M. Farid, M. Fakoor, Mixed mode I/II fracture criterion for arbitrary cracks in orthotropic materials considering T-stress effects, Theor. Appl. Fract. Mech. 99 (2019) 147–160.
[45] N.M. Khansari, M. Fakoor, F. Berto, Probabilistic micromechanical damage model for mixed mode I/II fracture investigation of composite materials, Theor. Appl. Fract. Mech. 99 (2019) 177–193.
[46] M. Fakoor, S. Shahsavar, The effect of T-stress on mixed mode I/II fracture of composite materials: reinforcement isotropic solid model in combination with maximum shear stress theory, Int. J. Solids Struct. (2021), 111145.
[47] M. Fakoor, S. Shahsavar, Fracture assessment of cracked composite materials: Progress in models and criteria, Theor. Appl. Fract. Mech. 105 (2020), 102430.
[48] M. Romanowicz, A. Seweryn, Verification of a non-local stress criterion for mixed mode fracture in wood, Eng. Fract. Mech. 75 (10) (2008) 3141–3160.
[49] A.G. Anaraki, M. Fakoor, Mixed mode fracture criterion for wood based on a reinforcement microcrack damage model, Mater. Sci. Eng., A 527 (27–28) (2010) 7184–7191.
[50] A.G. Anaraki, M. Fakoor, A new mixed-mode fracture criterion for orthotropic materials, based on strength properties, The Journal of Strain Analysis for Engineering Design 46 (1) (2011) 33–44.
[51] M. Fakoor, N.M. Khansari, Mixed mode I/II fracture criterion for orthotropic materials based on damage zone properties, Eng. Fract. Mech. 153 (2016) 407–420.
[52] J. Ju, On two-dimensinal self-consistent micromechanical damage models for brittle solids, Int. J. Solids Struct. 27 (2) (1991) 227–258.
[53] J. Ju, T.M. Chen, Micromechanics and effective moduli of elastic composites containing randomly dispersed ellipsoidal inhomogeneities, Acta Mech. 103 (1) (1994) 103–121.
[54] X. Feng, S. Yu, Estimate of effective elastic moduli with microcrack interaction effects, Theor. Appl. Fract. Mech. 34 (3) (2000) 225–233.
[55] Z. Daneshjoo, M. Shokrieh, M. Fakoor, R. Alderliesten, A new mixed mode I/II failure criterion for laminated composites considering fracture process zone, Theor. Appl. Fract. Mech. 98 (2018) 48–58.
[56] M. Shokrieh, Z. Daneshjoo, M. Fakoor, A modified model for simulation of mode I delamination growth in laminated composite materials, Theor. Appl. Fract. Mech. 82 (2016) 107–116.
[57] L. Yao, R. Alderliesten, M. Zhao, R. Benedictus, Bridging effect on mode I fatigue delamination behavior in composite laminates, Compos. A Appl. Sci. Manuf. 63 (2014) 103–109.
[58] E. Triki, B. Zouari, A. Jarraya, F. Dammak, Experimental investigation of the interface behavior of balanced and unbalanced E-glass/polyester woven fabric composite laminates, Appl. Compos. Mater. 20 (6) (2013) 1111–1123.
[59] Z. Daneshjoo, M. Shokrieh, M. Fakoor, A micromechanical model for prediction of mixed mode I/II delamination of laminated composites considering fiber bridging effects, Theor. Appl. Fract. Mech. 94 (2018) 46–56.
[60] Z. Daneshjoo, L. Amaral, R. Alderliesten, M. Shokrieh, M. Fakoor, Development of a physics-based theory for mixed mode I/II delamination onset in orthotropic laminates, Theor. Appl. Fract. Mech. 103 (2019), 102303.
[61] M. Shokrieh, A. Zeinedini, A novel method for calculation of strain energy release rate of asymmetric double cantilever laminated composite beams, Appl. Compos. Mater. 21 (3) (2014) 399–415.

[62] S.E. Stanzl-Tschegg, Microstructure and fracture mechanical response of wood, Int. J. Fract. 139 (3) (2006) 495–508.
[63] M. Fakoor, M.S. Khezri, A micromechanical approach for mixed mode I/II failure assessment of cracked highly orthotropic materials such as wood, Theor. Appl. Fract. Mech. 109 (2020), 102740.
[64] M. Fakoor, S.M.N. Ghoreishi, Failure Criterion for Mixed Mode Fracture of Cracked Wood Specimens, International Journal of Mechanical and Mechatronics Engineering 11 (7) (2017) 1371–1377.
[65] J.M. Mahishi, An integrated micromechanical and macromechanical approach to fracture behavior of fiber-reinforced composites, Eng. Fract. Mech. 25 (2) (1986) 197–228.
[66] M. F. Hibbs and W. L. Bradley, "Correlations between micromechanical failure processes and the delamination toughness of graphite/epoxy systems," in *Fractography of modern engineering materials: composites and metals*: ASTM International, 1987.
[67] W. M. Jordan and W. L. Bradley, "Micromechanisms of fracture in toughened graphite-epoxy laminates," in *Toughened composites*: ASTM International, 1987.
[68] S. Hashemi, A. Kinloch, J. Williams, Mechanics and mechanisms of delamination in a poly (ether sulphone)—fibre composite, Compos. Sci. Technol. 37 (4) (1990) 429–462.
[69] E.S. Greenhalgh, C. Rogers, P. Robinson, Fractographic observations on delamination growth and the subsequent migration through the laminate, Compos. Sci. Technol. 69 (14) (2009) 2345–2351.
[70] J. Bonhomme, A. Argüelles, J. Viña, I. Viña, Fractography and failure mechanisms in static mode I and mode II delamination testing of unidirectional carbon reinforced composites, Polym. Test. 28 (6) (2009) 612–617.
[71] H. Dębski, T. Sadowski, Modelling of microcracks initiation and evolution along interfaces of the WC/Co composite by the finite element method, Comput. Mater. Sci. 83 (2014) 403–411.
[72] L. Amaral, R. Alderliesten, R. Benedictus, Towards a physics-based relationship for crack growth under different loading modes, Eng. Fract. Mech. 195 (2018) 222–241.
[73] Z. Daneshjoo, M.M. Shokrieh, M. Fakoor, R. Alderliesten, D. Zarouchas, Physics of delamination onset in unidirectional composite laminates under mixed-mode I/II loading, Eng. Fract. Mech. 211 (2019) 82–98.
[74] T. Van der Put, A new fracture mechanics theory for orthotropic materials like wood, Eng. Fract. Mech. 74 (5) (2007) 771–781.
[75] M. Fakoor, H.M. Farid, Mixed-mode I/II fracture criterion for crack initiation assessment of composite materials, Acta Mech. 230 (1) (2019) 281–301.
[76] H.M. Farid, M. Fakoor, Mixed mode I/II fracture criterion to anticipate behavior of the orthotropic materials, Steel and Composite Structures 34 (5) (2020) 671–679.
[77] M. Fakoor, M.S. Shokrollahi, A new macro-mechanical approach for investigation of damage zone effects on mixed mode I/II fracture of orthotropic materials, Acta Mech. 229 (8) (2018) 3537–3556.
[78] F. Erdogan, G. Sih, On the crack extension in plates under plane loading and transverse shear, J. Basic Eng. 85 (4) (1963) 519–525.
[79] G.C. Sih, Strain-energy-density factor applied to mixed mode crack problems, Int. J. Fract. 10 (3) (1974) 305–321.
[80] G.C. Sih, P. Paris, G.R. Irwin, On cracks in rectilinearly anisotropic bodies, Int. J. Fract.Mech. 1 (3) (1965) 189–203.
[81] H. Manafi Farid, M. Fakoor, Matrix Reinforcement Coefficients Models for Fracture Investigation of Orthotropic Materials, Modares Mechanical Engineering 19 (11) (2019) 2811–2822.
[82] A.G. Anaraki, M. Fakoor, General mixed mode I/II fracture criterion for wood considering T-stress effects, Mater. Des. 31 (9) (2010) 4461–4469.
[83] T. Van der Put, "A new consistent theory of fracture mechanics of wood," *Website: www. dwsf. nl/downloads*, 2005.
[84] L. Amaral, R. Alderliesten, R. Benedictus, Understanding mixed-mode cyclic fatigue delamination growth in unidirectional composites: An experimental approach, Eng. Fract. Mech. 180 (2017) 161–178.
[85] C. R. Corleto and W. L. Bradley, "Mode II delamination fracture toughness of unidirectional graphite/epoxy composites," in *Composite Materials: Fatigue and Fracture, Second Volume*: ASTM International, 1989.
[86] V. Saouma, "Fracture Mechanics. Lecture Notes," Dept. of Civil Environmental and Architectural Engineering, University of Colorado, Boulder, USA, 2000.
[87] S. Shahsavar, M. Fakoor, F. Berto, Verification of reinforcement isotropic solid model in conjunction with maximum shear stress criterion to anticipate mixed mode I/II fracture of composite materials, Acta Mech. 231 (12) (2020) 5105–5124.
[88] E.E. Gdoutos, Fracture mechanics: an introduction, Springer Nature (2020).
[89] A.T. Zehnder, Fracture mechanics, Springer Science & Business Media, 2012.
[90] R. Thornburgh, A. Chattopadhyay, Unified approach to modeling matrix cracking and delamination in laminated composite structures, AIAA journal 39 (1) (2001) 153–160.
[91] M. Fakoor, R. Rafiee, Fracture investigation of wood under mixed mode I/II loading based on the maximum shear stress criterion, Strength Mater. 45 (3) (2013) 378–385.
[92] M. Gupta, R. Alderliesten, R. Benedictus, A review of T-stress and its effects in fracture mechanics, Eng. Fract. Mech. 134 (2015) 218–241.
[93] C. CORLETO, W. BRADLEY, and M. HENRIKSEN, "Correspondence between stress fields and damage zones ahead of crack tip of composites under mode I and mode II delamination," in *International Conference on Composite Materials, 6 th, and European Conference on Composite Materials, 2 nd, London, England*, 1987, p. 3.
[94] Z. Yosibash, Failure criteria for brittle elastic materials, in: Singularities in Elliptic Boundary Value Problems and Elasticity and Their Connection With Failure Initiation, Springer, 2012, pp. 185–220.
[95] G. Amrutharaj, K. Lam, B. Cotterell, Fracture process zone concept and delamination of composite laminates, Theor. Appl. Fract. Mech. 24 (1) (1995) 57–64.
[96] L. Amaral, D. Zarouchas, R. Alderliesten, R. Benedictus, Energy dissipation in mode II fatigue crack growth, Eng. Fract. Mech. 173 (2017) 41–54.
[97] S.M. Lee, Mode II delamination failure mechanisms of polymer matrix composites, J. Mater. Sci. 32 (5) (1997) 1287–1295.
[98] S.M. Lee, Mode II interlaminar crack growth process in polymer matrix composites, J. Reinf. Plast. Compos. 18 (13) (1999) 1254–1266.
[99] Z. Khaji and M. Fakoor, "A Semi-theoretical criterion based on the combination of strain energy release rate and strain energy density concepts (STSERSED): Establishment of a new approach to predict the fracture behavior of orthotropic materials," *Theoretical and Applied Fracture Mechanics*, p. 103290, 2022.
[100] J. Jamali, M. Mahmoodi, M. Hassanzadeh-Aghdam, J. Wood, A mechanistic criterion for the mixed-mode fracture of unidirectional polymer matrix composites, Compos. B Eng. 176 (2019), 107316.
[101] R. Su, H. Sun, Numerical solutions of two-dimensional anisotropic crack problems, Int. J. Solids Struct. 40 (18) (2003) 4615–4635.
[102] A. Kaddour, M.J. Hinton, P.A. Smith, S. Li, Mechanical properties and details of composite laminates for the test cases used in the third world-wide failure exercise, J. Compos. Mater. 47 (20–21) (2013) 2427–2442.
[103] L.E. Asp, A. Sjögren, E.S. Greenhalgh, Delamination growth and thresholds in a carbon/epoxy composite under fatigue loading, J. Compos. Tech. Res. 23 (2) (2001) 55–68.
[104] L. Asp, The effects of moisture and temperature on the interlaminar delamination toughness of a carbon/epoxy composite, Compos. Sci. Technol. 58 (6) (1998) 967–977.
[105] J.R. Reeder, A bilinear failure criterion for mixed-mode delamination, ASTM Spec. Tech. Publ. 1206 (1993) 303.
[106] Ross, Robert J.. Wood handbook: wood as an engineering material. v. 190, USDA Forest Service, Forest Products Laboratory, General Technical Report FPL-GTR-190, 2010.